Combustion and Flame 213 (2020) 87–97

Contents lists available at ScienceDirect

Combustion and Flame

journal homepage: www.elsevier.com/locate/combustflame

Facilitating Bayesian analysis of combustion kinetic models with artificial neural network

Jiaxing Wang[a,b], Zijun Zhou[a,b], Keli Lin[a,b], Chung K. Law[a,c], Bin Yang[a,b,*]

[a] Center for Combustion Energy and Department of Energy and Power Engineering, Tsinghua University, Beijing 100084, PR China
[b] Key Laboratory for Thermal Science and Power Engineering of MOE, Tsinghua University, Beijing 100084, PR China
[c] Department of Mechanical and Aerospace Engineering, Princeton University, Princeton, NJ 08544, USA

ARTICLE INFO

Article history:
Received 18 June 2019
Revised 21 November 2019
Accepted 21 November 2019

Keywords:
Inverse uncertainty quantification
Bayesian analysis
Markov chain Monte Carlo
Artificial neural network

ABSTRACT

Bayesian analysis provides a framework for the inverse uncertainty quantification (UQ) of combustion kinetic models. As the workhorse of the Bayesian approach, the Markov chain Monte Carlo (MCMC) methods, however, incur a substantial computational cost. In this work, a surrogate model is employed to improve the traditional MCMC algorithm. Specifically, the test errors of three typical surrogate models are compared, namely Polynomial Chaos Expansion (PCE), High Dimensional Model Representation (HDMR) and Artificial Neural Network (ANN); and ANN is shown to be a relatively more efficient surrogate model for the approximation of combustion reaction systems under extensive conditions. An inverse UQ method, which is the combination of the ANN and traditional MCMC method, and as such termed ANN–MCMC, is adopted. The calculation is performed on the methanol oxidation system and a series of ignition delay data are employed to optimize the rate coefficients of the kinetic model. The estimated posterior distributions of the rate coefficients and the model predictions using the ANN–MCMC are compared with the traditional MCMC methods, with the results showing that the ANN–MCMC can significantly reduce the computational cost needed for the MCMC algorithm, especially on the estimation of the posterior distributions of the input parameters. The rejection rate of the samples in a Markov chain is very high, especially for the calculation of the posterior distribution of less sensitive parameters, thus a large number of samples are needed to reach a desired accuracy for traditional MCMC process. While no samples are rejected when training the ANN surrogate model. Therefore, fewer original samples are needed to get a converged ANN surrogate, which can then generate a large number of low-cost ANN samples for a better accuracy of the MCMC process. The errors for the estimated posterior distributions using ANN–MCMC depend on the accuracy of converged ANN surrogates and more accurate results are obtained with improved settings of ANN. The ANN–MCMC is especially suitable to the computational systems when the computational ability is limited.

1. Introduction

With the aim to improve the predictive ability and robustness of combustion kinetic models, the method of inverse uncertainty quantification (UQ) was proposed [1,2] to constrain the space of combustion model parameters and reduce the uncertainties of model predictions using experimental measurements. The inverse UQ was firstly proposed by Frenklach and co-workers [3], who developed a series of optimization tools including the data collaboration method [4,5] and the solution mapping method [6,7], which were employed in the development of the GRI-Mech [8]. Sheen and Wang [9] developed the Method of Uncertainty Minimization using Polynomial Chaos Expansions (MUM-PCE), which could significantly reduce the computational cost spent on the model evaluations and was applied to the optimization of several combustion kinetic models [9-11]. Recently, Turányi and coworkers developed a new model optimization algorithm based on both direct and indirect measurements with the aim to optimize all Arrhenius parameters of the important reactions, not just A factors [12]. They have successfully optimized the kinetic models of hydrogen [12], ethanol [13] and ethane [14].

Besides these methods, the Bayesian approach [15–19], which provides a probabilistic view to the inverse UQ, has attracted considerable attention. It begins with assuming a sound mathematical description to prior distributions for unknown parameters and experiment uncertainties, builds the relations by Bayesian

* Corresponding author at: Center for Combustion Energy and Department of Energy and Power Engineering, Tsinghua University, Beijing 100084, PR China.
E-mail address: byang@tsinghua.edu.cn (B. Yang).

https://doi.org/10.1016/j.combustflame.2019.11.035
0010-2180/

equation, employs stochastic sampling of the deterministic model of a system by solving the dominant differential equations, and produces posterior distributions for the input parameters and model predictions. The workhorse of Bayesian approach are the methods of Markov chain Monte Carlo (MCMC), which are the construction of a Markov chain whose steps produce correlated samples from the conditional posterior distributions of the parameters with given experimental data. Although the MCMC algorithm has been applied in many areas of science and engineering [15], it remains to be a relatively time-consuming tool, especially for high-dimensional systems. Specifically, during the sampling process of MCMC, the generated sample has the probability of being either accepted or rejected, and a large number of samples are required for a Markov chain to achieve convergence. Consequently, the applications of the Bayesian methods have been restricted to some simple cases, such as the optimization of a single reaction [20,21], or a small reaction set [17,18,22,23]. While for a combustion kinetic system of larger molecules, Bayesian methods may be limited, so other methods should be considered [17,24].

As discussed above, the Bayesian approach is a popular inverse UQ method but requires a high computational cost for the analysis of complex kinetic models. A practical solution to accelerate the MCMC algorithm is to construct a mathematical surrogate replacing the original kinetic model, and then generate the samples needed for the MCMC process through the surrogate. In this way, the computational cost of traditional MCMC method can be significantly reduced. Many mathematical surrogate models have been developed, such as Gaussian Process(GP) Emulator [16,19], Polynomial Chaos Expansion (PCE) [25] High Dimensional Model Representation (HDMR) [26,27] and Artificial Neural Networks(ANN) [28], which have been applied in various areas [17,29,30]. Cai et al. [31] combined the sensitivity analysis based (SAB) surrogate with the MCMC algorithm, which was successfully applied to the optimization of reaction rate rules of normal alkanes from C7 to C11. It should be noted that the SAB method is a kind of local sensitivity analysis methods, which may lead to a misleading result for a nonlinear system with quite large uncertainty range [35]. As such, the MCMC methods have the potential to be accelerated using other surrogates that are more suitable for nonlinear reaction systems. Specifically, PCE is one of the most widely applied surrogates within combustion research area [2,16,32–35], with its basic functions being orthogonal polynomials. The prediction uncertainty can be directly deduced from the coefficients of the orthogonal polynomials, and consequently the computational cost of forward UQ calculation can be significantly reduced. This method has been applied by Najm et al. on the analysis of hydrogen-air combustion systems, including 0-D ignition and 1-D premixed flame simulation [36–39]. The method of HDMR is also a popular surrogate developed by Li et al. [26]. This method constructs a hierarchical expansion to describe the mapping relationship between model inputs and outputs, which can effectively accelerate the global sensitivity analysis [40]. HDMR has been extensively applied by Tomlin et al., on the analysis of the kinetic models of methane [27], cyclohexane [41], dimethyl ether [42] and n-butane [43]. The surrogate model of Artificial neural network (ANN), which can capture the nonlinear mapping relationship of an input-output system, has attracted considerable attentions in recent years [44,45]. For example, the multi-layer perceptron (MLP) feed-forward neural network, one of the most widely applied ANN methods [46], has been applied on the numerical simulation of turbulent flows and sensitivity analysis [28].

The performances of mathematical surrogates may have significant differences under various conditions. Consequently, the selection of an appropriate surrogate is the key step in the application of surrogate-based Bayesian methods on highly nonlinear kinetic models, which determines the accuracy and computational cost of these methods.

In this work, the predictive efficiency and accuracy of the three typical surrogate models (ANN, PCE, and HDMR) are compared, and the ANN surrogate is shown to be an efficient surrogate with acceptable predictive accuracy, especially when there exists a high nonlinearity in the parameter space. We thus applied the combination of the ANN and MCMC algorithms (termed ANN–MCMC hereafter) to the combustion kinetic model systems. The primary goal of this method is to reduce the computational cost of MCMC [30,47] and hence makes the Bayesian approach possible to be applied in the model optimization of complicated combustion kinetic systems. A methanol oxidation system with a series of ignition delay data is employed to compare the performance of ANN–MCMC and the traditional MCMC. The reasons for the advantage of ANN–MCMC over traditional MCMC methods are also discussed.

2. Methodology

It is necessary to distinguish original samples from surrogate samples used in this paper. Original samples represent the input-output sample pairs obtained by the kinetic model evaluations and surrogate samples represent the input-output sample pairs generated by the well-trained surrogate models.

2.1. The Bayesian approach

In the Bayesian framework, the model input parameters $\boldsymbol{x} = [x_1, x_2, \ldots, x_n]$ are to be calibrated with the experiment data $\boldsymbol{d}$. Based on the Bayesian equation, the relationship between $\boldsymbol{x}$ and $\boldsymbol{d}$ is given by:

$$p_{\text{post}}(\boldsymbol{x}|\boldsymbol{d}) = \frac{p_{\text{prior}}(\boldsymbol{x})\pi(\boldsymbol{x};\boldsymbol{d})}{\int p_{\text{prior}}(\boldsymbol{x})\pi(\boldsymbol{x};\boldsymbol{d})d\boldsymbol{x}} \propto p_{\text{prior}}(\boldsymbol{x})\pi(\boldsymbol{x};\boldsymbol{d}) \tag{1}$$

where the $p_{\text{prior}}(\boldsymbol{x})$ is the prior distribution, which quantifies the knowledge of the random variables based on the available information [25]. The $p_{\text{post}}(\boldsymbol{x}|\boldsymbol{d})$ is the posterior distribution, which quantifies the information of calibrated model parameters given the experiment data. The function $\pi(\boldsymbol{x};\ \boldsymbol{d})$ is the likelihood function, and is decided by the values and uncertainties of the experiment data as well as the simulated values. The uncertainties in the experiments are usually assumed to be independent, normally distributed random variables [17]. Consequently, the likelihood function can be formulated as a multiplicative error model:

$$\pi(\boldsymbol{x};\boldsymbol{d}) = \frac{1}{\prod_{i=1}^{N_d}\sqrt{2\pi\sigma_i{}^2}} exp\left[-\frac{1}{2}\sum_{i=1}^{N_d}\left(\frac{lny_i - lnd_i}{\sigma_i}\right)^2\right] \tag{2}$$

In this equation, N_d is the number of experiment data, d_i is the value of experimental measurement at a certain condition and σ_i is the corresponding uncertainty, and y_i is the ith simulated result. The value of $\pi(\boldsymbol{x};\ \boldsymbol{d})$ represents the density of a candidate parameter vector realization with given experiment data and uncertainties.

One of the most widely applied methods to the Bayesian equation is the MCMC approach. As one of the MCMC methods, the Metropolis–Hastings (MH) [48] algorithm is adopted in this work, which is to explore a complex multi-dimensional probability distribution using a pre-specified proposal distribution, coupled with an accept–reject step. More details about this algorithm can be found in [49]. In this work, the multivariate normal distribution is adopted as the proposal distribution. The MH-MCMC algorithm is summarized as follows: Generate a sample from that of the previous iteration within the support range of the posterior distribution, calculate the acceptance rate of this sample and generate a

Algorithm 1
The Metropolis–Hastings algorithm [48].

1. **Given:** data $\boldsymbol{d}$; prior distribution $p_{\text{prior}}(\boldsymbol{x})$; likelihood function $\pi(\boldsymbol{x};\boldsymbol{d})$; proposal $q(\boldsymbol{x}^*|\boldsymbol{x})$, the number of total steps T.
2. Initialize $\boldsymbol{x}^0$
3. **For** $i = 1$ to T **do**
4. Generate candidate $\boldsymbol{x}^*$ from the $q(\boldsymbol{x}^*|\boldsymbol{x}^i)$
5. If $\boldsymbol{x}^* \notin supp(p_{\text{post}}(\boldsymbol{x}|\boldsymbol{d}))$, then $\boldsymbol{x}^{i+1} = \boldsymbol{x}^i$;
6. If $\boldsymbol{x}^* \in supp(p_{\text{post}}(\boldsymbol{x}|\boldsymbol{d})), then$:
7. Compute the acceptance rate:
$$\alpha = \min\left[1, \frac{p_{prior}(\boldsymbol{x}*)\pi(\boldsymbol{x}*;\boldsymbol{d})q(\boldsymbol{x}^i|\boldsymbol{x}*)}{p_{prior}(\boldsymbol{x}^i)\pi(\boldsymbol{x}^i;\boldsymbol{d})q(\boldsymbol{x}*|\boldsymbol{x}^i)}\right]$$
8. Generate sample u from the uniform distribution from 0 to 1
9. If $u < \alpha$, $\boldsymbol{x}^{i+1} = \boldsymbol{x}*$; *else* $\boldsymbol{x}^{i+1} = \boldsymbol{x}^i$
10. **End**

random number to decide whether to accept or reject this sample, and repeat this process until reaching the convergence of the Markov chain. Details of this algorithm are given in Algorithm 1.

Although many algorithms have been proposed to accelerate the traditional MCMC method, such as the adaptive algorithm and delayed rejection [50], the rejection rate of the samples in a Markov chain is still quite high [19]. Consequently, we will apply the mathematical surrogates on MCMC, which can replace the original simulation process and generate surrogate samples efficiently.

2.2. Surrogate models

As the most widely applied ANN, the multilayer perceptron method (MLP) is adopted in this work. An MLP consists of three kinds of layers: the input, hidden and output layers. The nodes in the input layer represent the input parameters, the nodes in the output layer represent the model outputs, and the nodes in the hidden layers are the connections between the input and output layers. The one-hidden-layer MLP is employed, which is sufficient to approximate most of the continuous functions [51]. The Python package Pyrenn is employed to construct the ANN surrogate [52]. The back propagation (BP) algorithm [53] is adopted for the training process of ANN, and the Levenberg-Marquardt optimization algorithm is applied to accelerate the convergence of the training process [46].

The accuracy and efficiency of ANN have been compared to the other two surrogates: PCE and HDMR. PCE represents a collection of polynomial approximation methods. The point collocation method [54], which is the most suitable PCE methods for the high-dimensional system, is adopted. The Python package Chaospy is employed to construct the PCE surrogates [55]. The random sampling (RS)-HDMR method and the orthonormal polynomials constructed by Li et al. [26] are employed. The coefficients of polynomials in RS-HDMR functions are determined by Monte Carlo integration over the chosen samples. The correlation method developed by Li et al. [56] is adopted to improve accuracy by reducing the variance of the Monte Carlo integrand.

The original model simulations are carried out to generate the samples with input parameters (e.g., rate parameters) and model predictions (e.g., ignition delay time). Then the samples are splitted into training dataset and test dataset. The prediction error on test dataset directly reflects the accuracy of the surrogate model. The accuracy is represented by the relative error between outputs $\boldsymbol{y} = [y^1, .., y^N]$ of the test samples and the surrogate model predictions $\boldsymbol{y_{predict}} = [y^i_{predict}, \ldots, y^N_{predict}]$, where N denotes the number of sample points.

$$\text{re} = \frac{1}{\text{N}}\sum_{\text{i}}\left|\frac{y^i - y^i_{predict}}{y^i}\right| \tag{3}$$

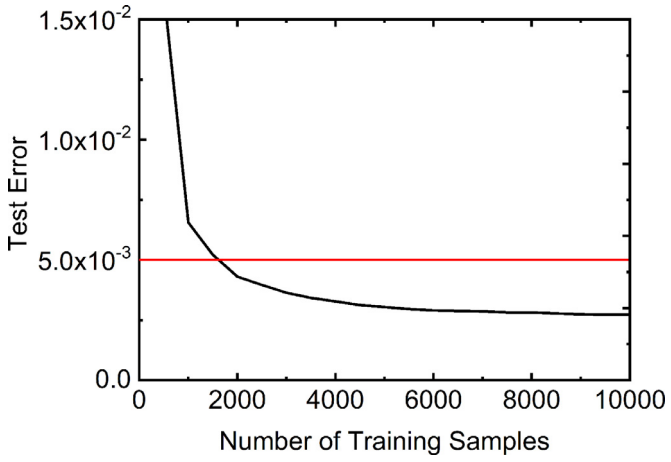

Fig. 1. The test error of a surrogate varies with the number of training samples.

The prediction accuracy of a surrogate increases if more training samples are included in the training dataset, and finally converges, as illustrated in Fig. 1. The converged accuracy of a surrogate should be lower than the desired accuracy. For kinetic simulations, the error of a surrogate with a value of 0.5% - 1% is satisfactory referring to the published UQ calculations [12,57]. In this work, the desired test error of a surrogate is thus selected as 0.5%. The efficiency of a surrogate is represented by the convergence speed for the test error curve. To make a quantitative comparison, the efficiency is decided by the number of training samples needed to reach the desired accuracy. The surrogate using fewer training sample is more efficient.

It should be noted that the training accuracy is also decided by the settings of the hyper-parameters of a surrogate. The performance of the PCE method is decided by the degrees of polynomial functions, and the polynomial degree is limited to be 3 [33]. The performance of RS-HDMR method is decided by the order of the component functions and the degree of the polynomial functions. The order of the component functions means the number of parameters contained in a term of the polynomial, (e.g., the order of $f(x_i)$ is 1, the order of $f(x_i, x_j)$ is 2, and so on). In this 0-D system, considering the first and second order component functions is accurate enough. In the first and second order component functions, the polynomial degree is limited to be 10 and 5, respectively. The performance of ANN is decided by the number of nodes in the hidden layer. The largest number of nodes in the hidden layer is set to be the number of input parameters. We have constructed surrogate models with different combinations of the hyper-parameters. The prediction accuracy and efficiency of these models are then compared to determine the optimal settings of all hyper-parameters. Each kind of surrogate is firstly adjusted to the optimal settings of hyper-parameters and then compared with other surrogates.

2.3. Surrogate model based MCMC method

Figure 2 shows the schematic of the surrogate model based MCMC method. The original samples are first generated from the kinetic simulations by solving the differential equations. Then surrogate models are constructed from the original samples under the simulated conditions, which are used as a mathematical approximation to the process of solving differential equations. The surrogate samples are generated from the surrogate model and an extremely long Markov chain can be generated because the computational cost to generate samples from the mathematical surrogate is much smaller than from the kinetic simulations. Then the

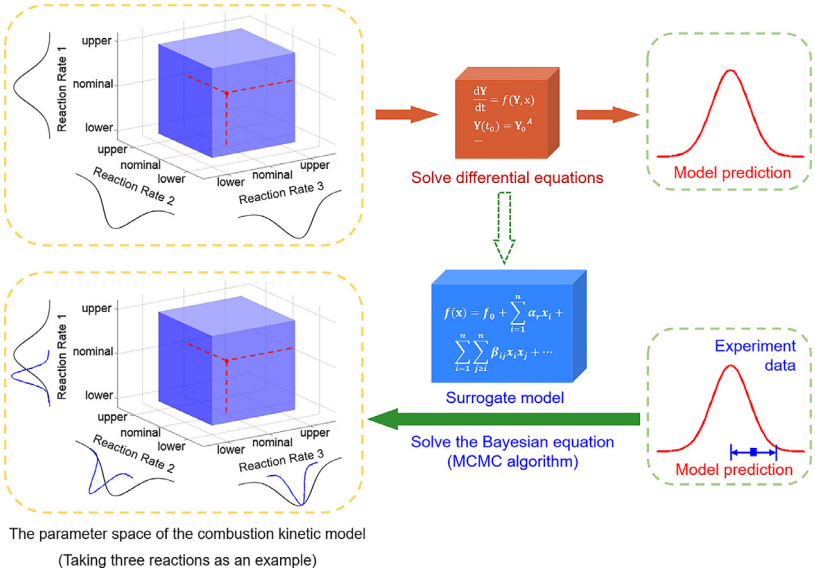

Fig. 2. The schematic of the surrogate model based MCMC method.

constrained parameter space can be calculated from the surrogate samples in the Markov Chains.

Modification of the kinetic model after optimization is reflected by the comparison of prior and posterior distributions of the input parameters (e.g., rate coefficient) and model predictions (e.g., ignition delay time). The prior model predictions are calculated from the Monte Carlo method, and the calculation process of this method has been introduced in [42]. The posterior model predictions are calculated from the samples in the Markov Chains. The marginal probability density function (PDF), the nominal value and standard deviation have been calculated to assess the prior and posterior distributions. The nominal value is calculated by the mean value of the simulated results. The standard deviation is estimated by the sample standard deviation of the simulated results.

3. Combustion kinetic model

The methanol oxidation model of Zhang et al. [58] is employed in this work, containing 212 input parameters (the pre-exponential factors of reactions). The uncertainty factor (UF) for a reaction rate is given by:

$$F = \frac{k_0}{k_{min}} = \frac{k_{\max}}{k_0} \tag{4}$$

where k_0 is the nominal value of the rate coefficient, and $k_{\max}$ and k_{min} are the upper and lower bounds of the rate coefficient, respectively. Each rate coefficient k_i is assumed to follow a prior log-uniform distribution within the uncertainty range $[k_{min}, k_{max}]$. The uncertainty factors of the rate coefficients were estimated from the literature compilations [59-61]. The kinetic models and uncertainty factors for this mechanism are listed in Table S1 in the *Supplementary material*. The high- and low-pressure limits of a fall-off reaction are regarded as different parameters. In this study, the A-factor in the reaction rate expression is taken as the input parameter. The aim of this study is to compare different model optimization methods, and the similar conclusion is drawn if other rate parameters are included. To reduce the calculation effort, reactions are screened based on the brute force linear sensitivity approach at the simulated conditions. This approach is achieved by increasing all the A-factors by 10% from their nominal values and the reactions which result in >1% change in the model response are selected. A total number of 33 reactions are selected.

Three groups of ignition delay time data [62] in the range of P = 10–50 atm and T = 994–1425 K are adopted for the model optimization. Both the experimental data and corresponding uncertainty factors are given in Table 1. The kinetic simulation is conducted on the Cantera platform [63]. The ignition simulation is conducted using the constant volume, adiabatic, zero-dimensional reactor. The ignition delay time is defined as the time of the difference in the moments between the rising and the maximum change rate of OH concentration. It is noted that the Bayesian approach is not restricted to a single type of experiment. Experiment data such as flame speeds and species mole fractions can also be included in this process. The ignition delay times are selected because they are quantified with relatively low uncertainties.

4. Results and discussion

4.1. Performances of different surrogates

The performances of PCE, HDMR and ANN surrogates are compared in this section. Figure 3 shows the test errors of these three surrogates with different settings. A training dataset with kinetic model evaluations up to 50,000 by Monte Carlo method is used, and by the same sample-generating method, a test dataset with 4000 kinetic model evaluations is used to calculate the test errors. The simulated target for each surrogate is the ignition delay time of CH_3OH under the condition of T = 998 K, P = 20.358 atm and φ = =2. It can be seen that for the three surrogates the test errors decrease as the original sample size of the training dataset increases and converges to specific values with sufficient samples. It is also noted that the convergence speed and converged test error are quite different for these surrogates.

Figure 3(a) shows the test error curves of the PCE surrogates with different polynomial degrees. It is seen that the test errors of PCE converge to a lower value with increasing polynomial degree. For example, the second-degree PCE can reach a relative error of 0.3%, while the first-degree PCE can only converge to around 1%. The results indicate that the accuracy of the PCE surrogate increases with the complexity of the surrogate. However, for a higher-degree PCE function, more original samples are usually needed to reach convergence. By comparison, a third-degree PCE needs more than 15,000 original samples to converge, while the second-degree PCE needs only 1000 original samples. It is also

Table 1
The experimental data [62] and corresponding uncertainty factors.

Index	*P*/atm	*T*/K	Species composition	Ignition delay time/ms	UF
1	20.358	998.0	CH_3OH:0.05,O_2:0.15,N_2:0.80	1.4304	0.2
2	20.154	1038.7	CH_3OH:0.05,O_2:0.15,N_2:0.80	0.7384	0.2
3	20.487	1096.8	CH_3OH:0.05,O_2:0.15,N_2:0.80	0.2984	0.2
4	20.061	1117.8	CH_3OH:0.05,O_2:0.15,N_2:0.80	0.2444	0.2
5	20.188	1155.5	CH_3OH:0.05,O_2:0.15,N_2:0.80	0.1544	0.2
6	19.978	1184.9	CH_3OH:0.05,O_2:0.15,N_2:0.80	0.1124	0.2
7	19.632	1214.0	CH_3OH:0.05,O_2:0.15,N_2:0.80	0.0844	0.2
8	19.877	1061.5	CH_3OH:0.05,O_2:0.15,N_2:0.80	0.6084	0.2
9	19.988	1068.8	CH_3OH:0.05,O_2:0.15,N_2:0.80	0.4400	0.2
10	19.269	1240.4	CH_3OH:0.05,O_2:0.15,N_2:0.80	0.0660	0.2
11	49.362	998.9	CH_3OH:0.057,O_2:0.0855,AR:0.8575	1.0570	0.2
12	49.930	1054.1	CH_3OH:0.057,O_2:0.0855,AR:0.8575	0.4619	0.2
13	51.149	1295.6	CH_3OH:0.057,O_2:0.0855,AR:0.8575	0.0296	0.2
14	50.023	994.5	CH_3OH:0.057,O_2:0.0855,AR:0.8575	1.1130	0.2
15	45.436	1136.3	CH_3OH:0.057,O_2:0.0855,AR:0.8575	0.1580	0.2
16	9.740	1090.6	CH_3OH:0.031,O_2:0.0465,AR:0.9225	1.3333	0.2
17	10.383	1183.5	CH_3OH:0.031,O_2:0.0465,AR:0.9225	0.5292	0.2
18	10.400	1236.0	CH_3OH:0.031,O_2:0.0465,AR:0.9225	0.2817	0.2
19	10.031	1260.7	CH_3OH:0.031,O_2:0.0465,AR:0.9225	0.2309	0.2
20	10.047	1312.9	CH_3OH:0.031,O_2:0.0465,AR:0.9225	0.1446	0.2
21	10.063	1365.3	CH_3OH:0.031,O_2:0.0465,AR:0.9225	0.0912	0.2
22	10.178	1425.8	CH_3OH:0.031,O_2:0.0465,AR:0.9225	0.0485	0.2

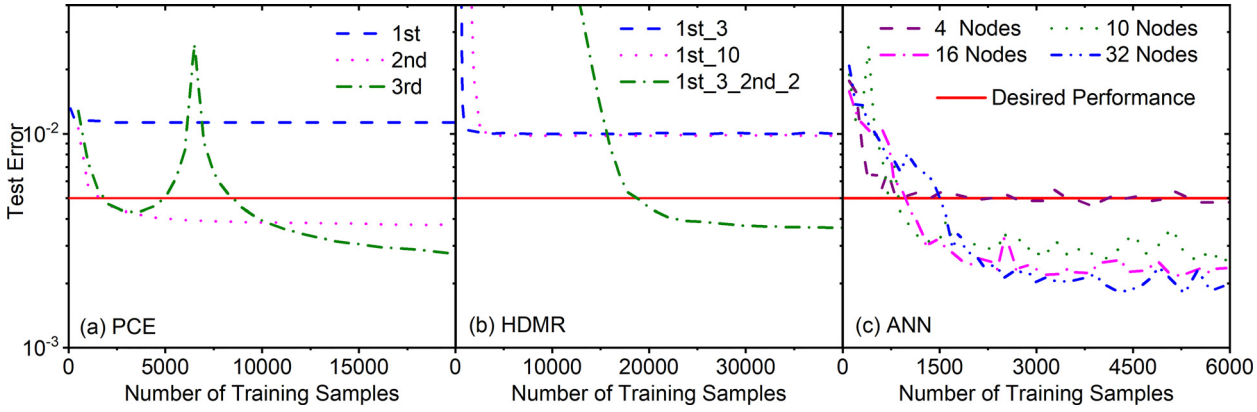

Fig. 3. The predicting accuracy of various surrogates trained with different numbers of original samples. (a) The test error of PCE surrogates with different polynomial degrees. (b) The test error of RS-HDMR surrogates with different component orders and polynomial degrees. '1st_3_2nd_2' represents the RS-HDMR surrogate with two orders of component functions and the polynomial degree of the first and second order component function is 3 and 2. (c) The test errors of one-hidden-layer ANN surrogates with different numbers of nodes in the inner layer.

noted that the training of a structure-complicated surrogate may require large-size original samples to produce reliable results. For example, the test error of the third-degree PCE trained with 6000 original samples is larger than those trained with fewer original samples. Consequently, for the case studied in this work, a second-degree PCE is selected, which can reach a satisfactory accuracy but needs far fewer original samples than the third-degree PCE.

The performance of the HDMR surrogate is decided by the orders of the component functions and the degrees of the polynomials used at each level of the component function. As shown in Fig. 3(b), the test errors for two RS-HDMR surrogates with first-order component functions (marked by '1st_3' and '1st_9') and one RS-HDMR surrogate with second-order component functions (marked by '1st_3_2nd_2') are plotted. Here, '1st_3' represents the RS-HDMR function which has only the first-order component function and the polynomial degree on this function is 3; '1st_3_2nd_2' represents the RS-HDMR function which has two orders of component functions, and the polynomial degrees on the first and second order component function are 3 and 2, respectively. The order of component functions is dominant for the accuracy of the RS-HDMR method. It is hard to reach the desired accuracy for an RS-HDMR with only first-order component function, while it can reach the desired accuracy for an RS-HDMR function with even the simplest second-order component functions (using only second-degree polynomials). However, at least 20,000 original samples are needed for the training process, which is less efficient than the PCE method.

The model complexity of the ANN surrogate is proportional to the number of nodes in the hidden layer. As shown in Fig. 3(c), the one-hidden-layer ANN with nodes larger than 10 is easy to reach a test error less than the desired 0.5%. ANN can converge to a lower test error by increasing the number of nodes in the hidden layer at the cost of more original samples needed for the training dataset. Only 1500 original samples are needed to train ANN surrogates with 10 nodes to reach the desired performance, while the training cost is higher for ANN surrogates with more nodes.

It is noted that all the three types of surrogates can converge to the desired test error, as long as the structure of each surrogate is set to be complex enough; for higher degree of polynomials for example. However, these three surrogates have different training efficiencies. For example, for the case studied here, the HDMR, PCE and ANN surrogates need nearly 20,000, 1700 and 1200 original samples to reach the test error of less than 0.5%, respectively. The results from Fig. 3 suggest that ANN is far more efficient than

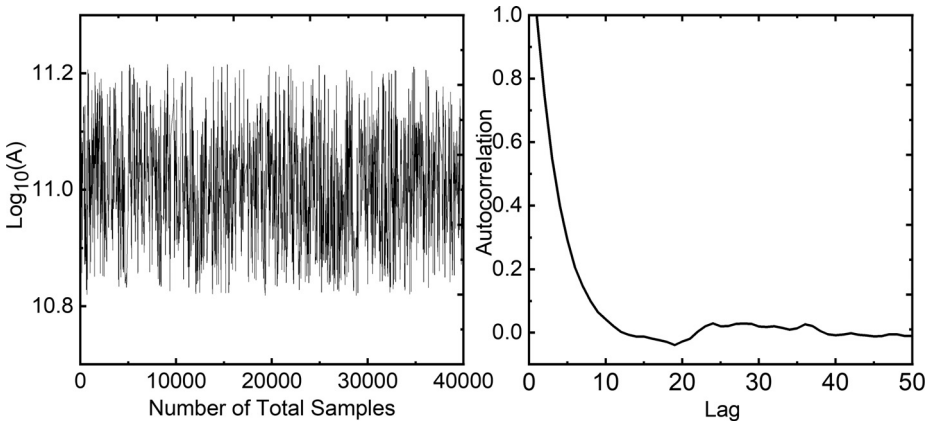

Fig. 4. The subsection of sampling results (the left panel) and autocorrelation for the O + +H_2==H+OH pre-exponential coefficient (the right panel).

HDMR and slightly more efficient than PCE to approximate these systems. Moreover, the ANN surrogate is good at catching the nonlinear input-output relationship. The test error of ANN surrogate can be lower than that of PCE or HDMR under the conditions with a high order of non-linear effects. To further compare the performances of ANN, HDMR, and PCE, the test errors of these three surrogates are also calculated in the combustion reaction systems of hydrogen and butane. In addition, the species mole fraction in methanol premixed flame is also selected as the target. The detailed discussion is given in the *Supplementary Material*. In general, the ANN surrogate shows the best performances for both low and high dimensional systems. Particularly, for the hydrogen system at the condition where there is a higher order nonlinear effect (e.g., Fig. S1), the accuracy of PCE and HDMR methods is much worse compared to the ANN surrogate, because ANN is better at catching the nonlinear input-output relationship [64,65]. The basic functions of PCE and RS-HDMR are both polynomial expansions, but these two methods differ in the training methods. The PCE surrogate is trained by the linear regression method, while the RS-HDMR surrogate by the Monte Carlo integration method. The basic function of ANN is the sigmoid function, which has the characteristic 'S'-shaped curve and thus favors catching the nonlinear relationship. Consequently, the ANN surrogate can approximate the combustion system more accurately and converge to a relatively lower test error, and is selected as the surrogate model to be combined with the MCMC algorithm in the next section.

4.2. Comparison of MCMC and ANN–MCMC

The ANN–MCMC model optimization method, which is the combination of ANN surrogate with the traditional MCMC algorithm, is applied in this work. The performances of ANN–MCMC and traditional MCMC method are compared in this section. First, we get the optimized results of the model parameters by taking the mean value of the posterior distribution. The optimized results of A-factors using the traditional MCMC method regardless of computational cost are given, which are further used as the benchmarks to evaluate the performance of ANN–MCMC. Then the optimized results calculated by ANN–MCMC and MCMC using various numbers of original samples are compared with the benchmarks, with the aim to assess the accuracy and efficiency of these two methods with lower computational cost.

4.2.1. Model optimization based on traditional MCMC

Results of the traditional MCMC are given in this section, including the posterior marginal PDFs of rate parameters and model predictions. A Markov chain with 50,000 original samples based on the traditional MCMC is generated, which is further used as a benchmark to assess the performance of ANN–MCMC. The convergence of this Markov chain was checked by the trace and autocorrelation plots [17], as shown in Fig. 4. The chain itself shows reasonable mixing and the autocorrelation dies out fast within 20 samples, which indicates that this Markov chain has attained convergence under this condition [17,66].

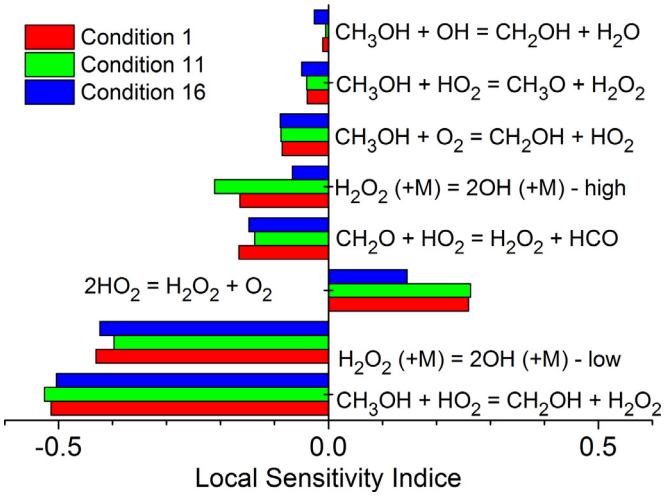

Fig. 5. The local sensitivity indices of the most sensitive 8 reactions. The simulated conditions (1, 11 and 16) are in accordance with the index given in Table 1.

The rate coefficients of the reactions in the kinetic model may be optimized by the Bayesian UQ analysis, and the marginal PDF of the rate parameters can be compared before and after the model optimization. Reactions with relatively large local sensitivity indice after model optimization are given in Fig. 5. As can be seen, several reactions related to H_2O_2 and HO_2 are very sensitive to the ignition delay predictions under the selected conditions: CH_3OH+ + HO_2= = CH_2OH + +H_2O_2, H_2O_2 (+M)= = 2OH (+M) and $2HO_2$= = H_2O_2+ + O_2. Figure 6 shows the comparison of prior and posterior marginal PDFs for the pre-exponential factors of the two most sensitive reactions: CH_3OH+HO_2= = CH_2OH + +H_2O_2 and the low-pressure limit of H_2O_2(+M)= = 2OH(+M). The deviation between the prior distributions (marked by dashed lines) and the posterior distributions (marked by solid lines) of these two rate parameters are larger than those of other reactions. Both of these two reactions need to have larger rate coefficients in order to reproduce the experimental data better. For the reactions that are relatively less sensitive to the prediction targets, the distributions of rate parameters are only slightly changed, as seen in Fig. 7.

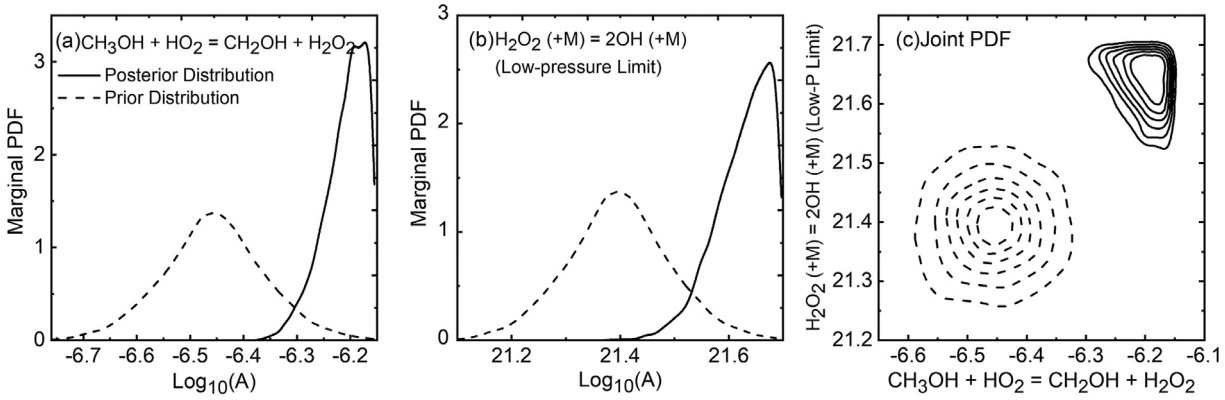

Fig. 6. The prior and posterior marginal PDFs for the pre-exponential factors of two reactions: (a) $CH_3OH+HO_2= = CH_2OH+H_2O_2$ and (b) the low-pressure limit of $H_2O_2(+M)= = 2OH$ and (c) the two-dimensional marginal joint PDF for the pre-exponential factors of these two reactions. The results are based on the MCMC approach with 50,000 original samples.

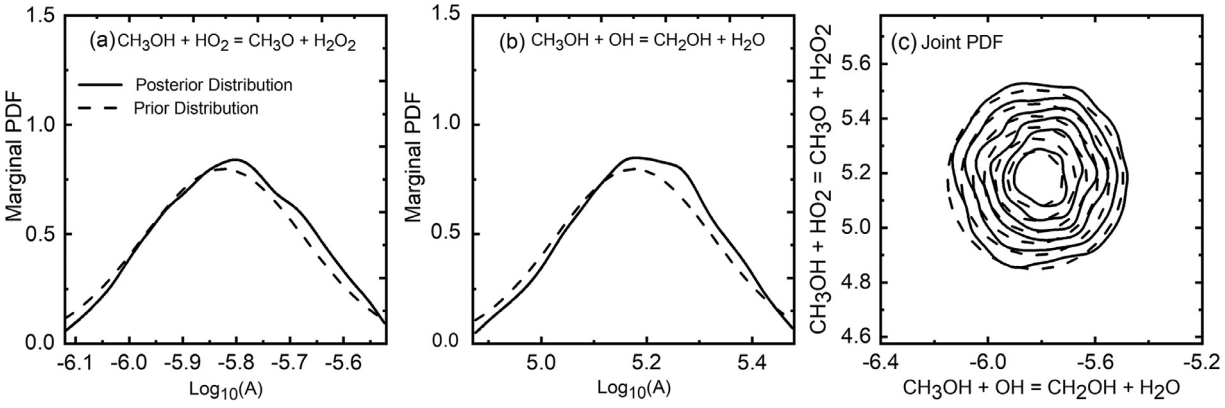

Fig. 7. The prior and posterior marginal PDFs for the pre-exponential factors of two reactions: (a) $CH_3OH+ + HO_2= = CH_3O+ + H_2O_2$ and (b) $CH_3OH+ + OH= = CH_2OH+ + H_2O$ and (c) the two-dimensional marginal joint PDF for the pre-exponential factors of these two reactions. The results are based on the MCMC approach with 50,000 original samples.

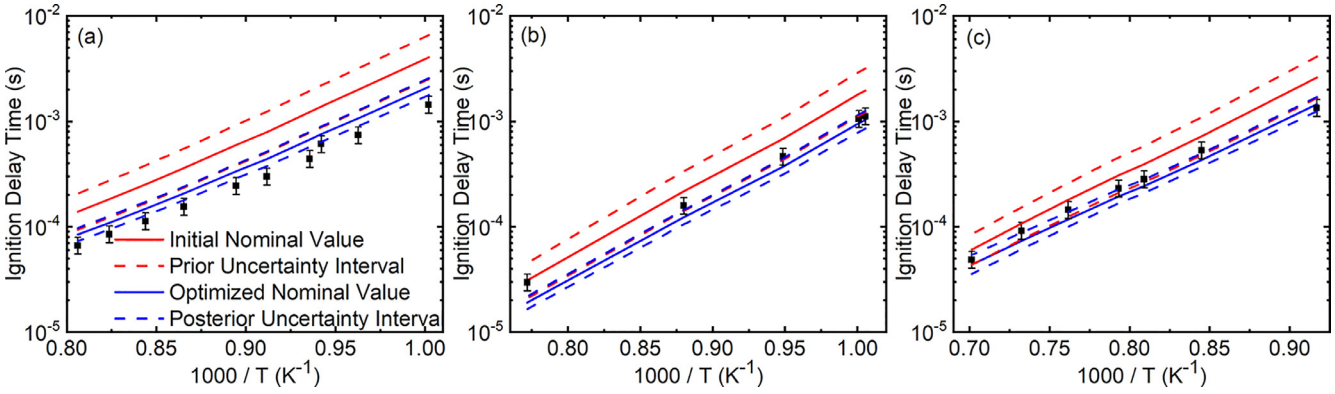

Fig. 8. The prior and posterior distributions for the model predictions of the ignition delay time under conditions 1(a), 11(b) and 16(c). The results are based on the MCMC approach with 50,000 original samples.

The posterior model predictions (i.e. ignition delay times) can be estimated from the simulated predictions of the samples in a Markov chain. The prior and posterior model predictions including the nominal values and uncertainty intervals for the simulated ignition times are shown in Fig. 8. The values of the experimental data, as well as the corresponding uncertainty intervals, are also marked in the figure. It is noted that, with increasing temperature, predictions of the model have the same trend with the experiment data, but the model generally overestimates the ignition delay times under the selected conditions. Based on the Bayesian calibration, the optimized kinetic model can well predict these experimental data within the uncertainty interval.

4.2.2. ANN–MCMC versus MCMC

In this section, the performances of ANN–MCMC and traditional MCMC are compared with the benchmarks given above. The posterior distributions of the rate coefficients by ANN–MCMC and MCMC using different numbers of original samples are calculated. In the process of ANN–MCMC, ANNs are trained with different sizes of training samples from 100 to 30,000 under each simulated condition. Then Markov chains are constructed with 50,000 surro-

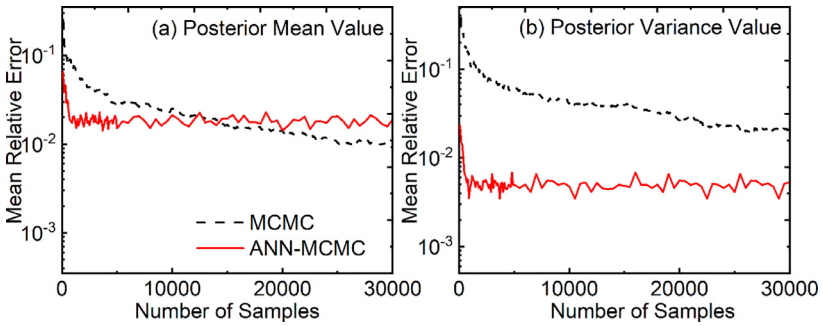

Fig. 9. The mean relative errors for (a) the means and (b) variances of all the posterior reaction rates based on the MCMC and ANN–MCMC calculation using different numbers of original samples.

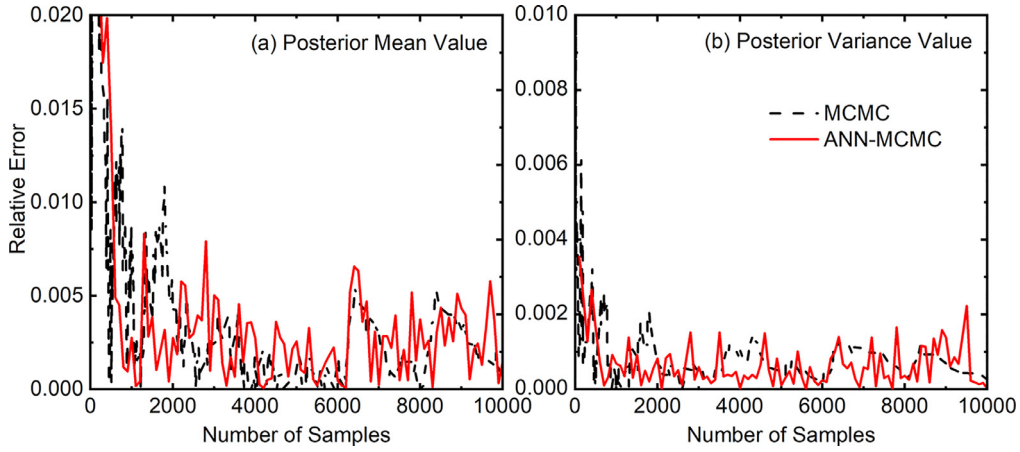

Fig. 10. The relative errors for (a) the mean and (b) variance of the posterior reaction rate of $CH_3OH+ + HO_2= = CH_2OH+ + H_2O_2$ based on the MCMC and ANN–MCMC calculation using different numbers of original samples. Here the benchmarks are the posterior mean and variance of the rate parameter which are calculated using the traditional MCMC method with 50,000 original samples given in Section 4.2.1.

gate samples generated from the trained ANNs, and the posterior distributions for input parameters are calculated from these chains. The nubmer of nodes in the hidden layer of ANN is set to be half of the number of the input parameters.

To make an overall comparison of these two methods, the mean relative errors of the posterior mean and variance for all the model parameters are calculated. From the view of all the input parameters, ANN–MCMC can reach a similar accuracy using much fewer original samples than MCMC. As shown in Fig. 9(a), the posterior means of reaction rates based on ANN–MCMC using 700 original samples can reach an accuracy near 1%, but the MCMC method needs nearly 10,000 original samples to reach such an accuracy. The higher efficiency using ANN is more obvious in the calculation of the posterior variance. It is seen in Fig. 9(b) that the posterior variance of ANN–MCMC with 700 original samples is better than that of the MCMC with 30,000 original samples. The application of ANN can reduce the original samples needed to reach a specific accuracy for an optimized model, which thus proceeds the calculation of the posterior variance more significantly. It is noted that the error of ANN–MCMC is not reduced with more original samples included once the structure is fixed, while the traditional MCMC method can be more accurate when sufficient original samples are provided.

The computational cost of the kinetic simulation is usually much higher than other processes such as MCMC optimization and ANN construction. The computational time spent on the different computational processes of ANN–MCMC with 700 original samples and 50,000 surrogate samples and MCMC with 10,000 original samples is compared. The calculation is conducted on a computer with an Intel(R) Core(TM) i7-6700 processor (4.00 GHz) and memory of 64 Gbytes. As given in Table 2, for both methods, most of the computational time is through the process of kinetic model evaluations. The additional computational time through the application of ANN, including the time spent on training ANN and ANN model evaluations, contributes less than 15% of the entire process. The application of the ANN surrogate model can effectively reduce the need for kinetic model evaluations, replacing most of them with ANN model evaluations. According to the analysis of Lu and Law [67], the computational cost for the simulation of the chemical reacting flow increases exponentially with the number of species. As such, the ANN–MCMC method will be more effective if applied to larger kinetic models.

Table 2
The computational time spent on ANN–MCMC with 700 original samples and 50,000 surrogate samples verses MCMC with 10,000 original samples.

	MCMC	ANN–MCMC
Kinetic model evaluations	40735 s	2851 s
Training of ANNs	–	314 s
ANN model evaluations	–	130 s
MCMC process	270 s	336 s
All	41005 s	3632 s

4.2.3. Explanation of the performances of ANN–MCMC and MCMC

In the traditional MCMC process, the input parameters which influence model predictions most significantly, i.e. with the highest sensitivity indices, will be modified first, because the adjustment of those important parameters can attain a high acceptance rate and the new samples can be easily accepted in a Markov chain. Figure 10 shows the relative errors for the optimized rate parameter of $CH_3OH+ + HO_2= = CH_2OH+ + H_2O_2$ calculated by

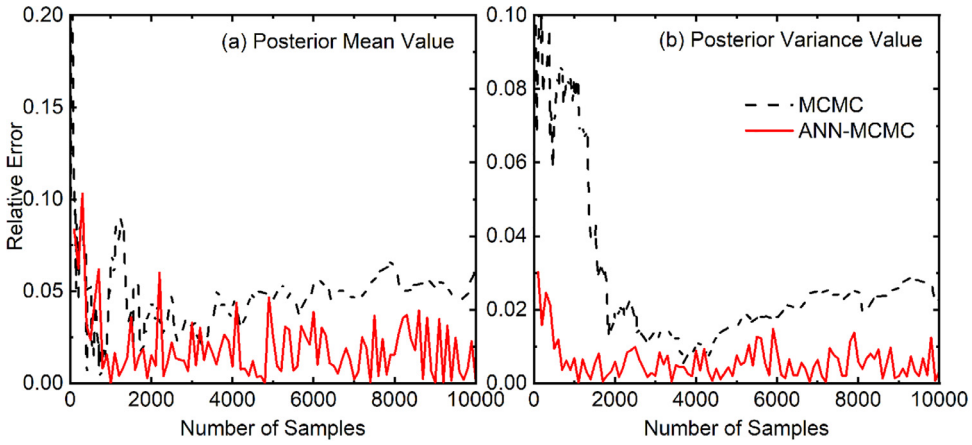

Fig. 11. The relative errors for (a) the means and (b) variances of the posterior reaction rate of $CH_3OH+ + HO_2= = CH_3O+ + H_2O_2$ based on the MCMC and ANN–MCMC calculation using different numbers of original samples.

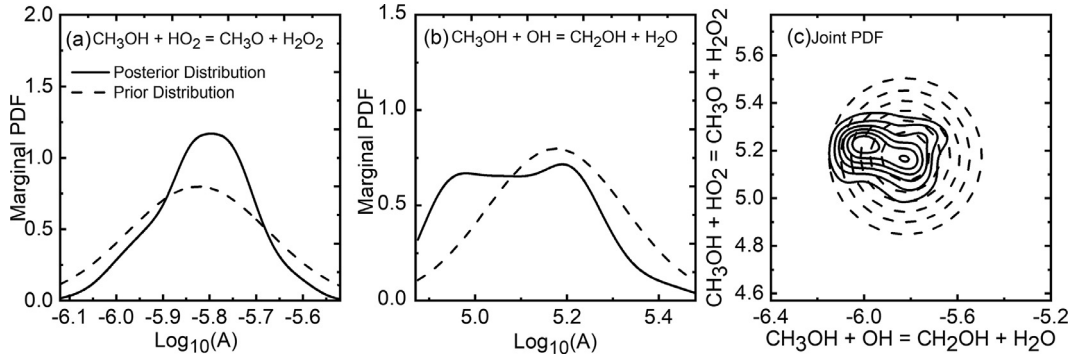

Fig. 12. The prior and posterior marginal PDFs for the pre-exponential factors of two reactions: (a) $CH_3OH+ + HO_2= = CH_3O+ + H_2O_2$ and (b) $CH_3OH+ + OH= = CH_2OH+ + H_2O$ and (c) the two-dimensional marginal joint PDF for the pre-exponential factors of these two reactions. The results are based on the MCMC approach with 700 original samples.

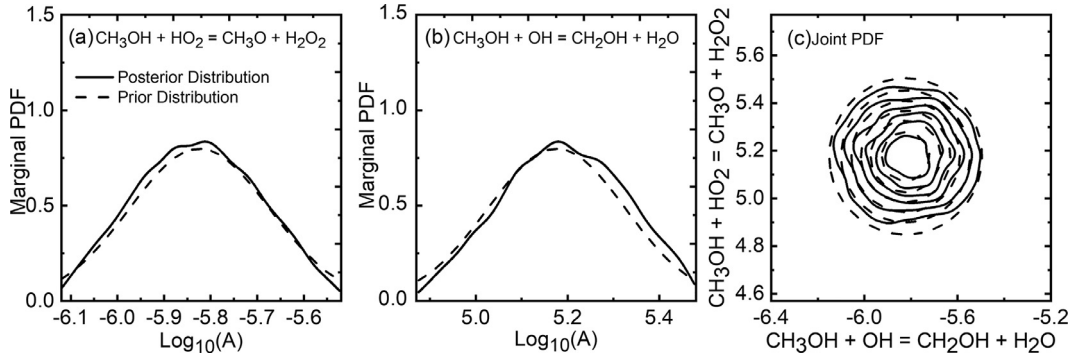

Fig. 13. The prior and posterior marginal PDFs for the pre-exponential factors of two reactions: (a) $CH_3OH+ + HO_2= = CH_3O+ + H_2O_2$ and (b) $CH_3OH+ + OH= = CH_2OH+ + H_2O$ and (c) the two-dimensional marginal joint PDF for the pre-exponential factors of these two reactions. The results are based on the ANN–MCMC approach with 700 original samples.

the MCMC and ANN–MCMC with different numbers of original samples. This reaction is the most sensitive one in this case. It is seen that the relative errors calculated using these two methods are both fast converged to be less than 1%, and the results of MCMC and ANN–MCMC are nearly the same. However, there are larger random errors for the estimation of those "less sensitive" parameters, especially when the original samples included in the traditional MCMC process are not sufficient. Figure 11 shows the relative errors for the posterior mean and variance of the rate constant for $CH_3OH+ + HO_2= = CH_3O+ + H_2O_2$ calculated by MCMC and ANN–MCMC. $CH_3OH+ + HO_2= = CH_3O+ + H_2O_2$ is less sensitive compared with $CH_3OH+ + HO_2= = CH_2OH+ + H_2O_2$. This lower sensitivity brings the obstacle to the traditional MCMC methods to calculate the posterior distribution of the rate constant resulting from a low acceptance rate while sampling. On the contrary, no samples are rejected when training the ANN surrogate model. It is seen that the relative errors of ANN–MCMC are smaller than MCMC with the original training samples less than 10,000. Furthermore, the ANN–MCMC method can reach a relative error near 10^{-3} for the estimation of posterior variance value, while the MCMC method can only reach a value larger than 10^{-2}. The application of ANN can generate a much larger number of surrogate samples (50,000 in this work) with lower computational cost, which contributes to reducing the random error in the MCMC

process. In this way, the ANN–MCMC can calculate the posterior distribution more accurately with fewer original samples.

We now conduct a detailed comparison between the posterior distribution calculated by ANN–MCMC and MCMC. Figures 12 and 13 show the posterior marginal PDFs for the rate parameters of $CH_3OH+ + HO_2= = CH_3O+ + H_2O_2$ and $CH_3OH+ + OH= = CH_2OH+ + H_2O$. It is seen that 700 kinetic model evaluations are insufficient for the traditional MCMC to estimate the distributions of these two parameters, which yields the calculated posterior marginal PDFs (in Fig. 12) that are obviously different from the benchmarks (shown in Fig. 7). However, these kinetic model evaluations are sufficient to construct the ANN surrogates with a prediction error of less than 1%. The converged Markov chain (including 50,000 surrogate samples), which is constructed using the samples from ANNs, can exclude the influence of the random errors and provide almost the same estimation of posterior distributions (in Fig. 13) as the benchmarks.

5. Conclusion

The key question for the development of the surrogate-based MCMC method is to find an efficient and accurate surrogate model. The test errors of three typical surrogates, namely PCE, HDMR and ANN, have been compared using a methanol reaction system. The surrogates with more complicated structures, e.g., higher degrees of polynomials and more nodes in the hidden layer, tend to converge to lower test errors at the cost of using more training samples. The ANN surrogate model shows better efficiency for the systems studied in this work compared to the other two methods under the selected conditions, and ANN is thus chosen as the surrogate to facilitate Bayesian analysis. Results show that ANN–MCMC can significantly reduce the original samples needed and thus the computational time compared to MCMC to reach the desired accuracy. Under the studied conditions, ANN–MCMC with 700 original samples has nearly the same performances as MCMC with more than 10,000 original samples. The computational time of the ANN–MCMC method is about one tenth of that of the traditional MCMC method. The MCMC process usually requires a large size of samples to reach a required accuracy for the posterior parameters, because the rejection rate of the samples in a Markov chain is very high, particularly for the calculation of the posterior distribution of less sensitive parameters. However, no samples are rejected when training the ANN surrogate models. Therefore, we can use fewer original samples to get a converged ANN surrogate and then use a very large number of ANN samples to get a better accuracy of the MCMC process.

In order to further improve the efficiency of the ANN–MCMC method, some efficient sampling methods such as Sobol's sequence and Latin Hypercube sampling [35] can be used to accelerate the convergence of ANN, which, however, cannot be applied in traditional MCMC. In addition, the ANN surrogate under each condition can also be constructed independently, so the ANN–MCMC method can be easily combined with parallel computational methods.

Declaration of Competing Interest

The authors declare that they have no known competing financial interests or personal relationships that could have appeared to influence the work reported in this paper.

Acknowledgment

This study was supported by the National Natural Science Foundation of China (Grant No. 91741109) and the Joint Fund of the National Natural Science Foundation of China and the Chinese Academy of Sciences (Grant No. U1832192).

Supplementary materials

Supplementary material associated with this article can be found, in the online version, at doi:10.1016/j.combustflame.2019.11.035.

References

[1] M. Frenklach, H. Wang, M.J. Rabinowitz, Optimization and analysis of large chemical kinetic mechanisms using the solution mapping method—combustion of methane, Prog. Energy Combust. Sci. 18 (1992) 47–73.
[2] H. Wang, D.A. Sheen, Combustion kinetic model uncertainty quantification, propagation and minimization, Prog. Energy Combust. Sci. 47 (2015) 1–31.
[3] M. Frenklach, Systematic optimization of a detailed kinetic model using a methane ignition example, Combust. Flame 58 (1984) 69–72.
[4] X. You, A. Packard, M. Frenklach, Process informatics tools for predictive modeling: hydrogen combustion, Int. J. Chem. Kinet. 44 (2012) 101–116.
[5] X. You, T. Russi, A. Packard, M. Frenklach, Optimization of combustion kinetic models on a feasible set, Proc. Combust. Inst. 33 (2011) 509–516.
[6] T. Yuan, C. Wang, C.L. Yu, M. Frenklach, M.J. Rabinowitz, Determination of the rate coefficient for the reaction $H + O_2 \rightarrow OH + O$ by a shock tube/laser absorption/detailed modeling study, J. Phys. Chem. 95 (1991) 1258–1265.
[7] B. Eiteneer, M. Frenklach, Experimental and modeling study of shock-tube oxidation of acetylene, Int. J. Chem. Kinet. 35 (2003) 391–414.
[8] G.P. Smith, D.M. Golden, M. Frenklach, N.W. Moriarty, B. Eitenee, M. Goldenberg, C.T. Bowman, R.K. Hanson, S. Song, W.C. Gardiner, V.V. Lissianski Jr., Z. Qin, available at <http://www.me.berkeley.edu/gri_mech/>.
[9] D.A. Sheen, H. Wang, Combustion kinetic modeling using multispecies time histories in shock-tube oxidation of heptane, Combust. Flame 158 (2011) 645–656.
[10] D.A. Sheen, C.M. Rosado-Reyes, W. Tsang, Kinetics of h atom attack on unsaturated hydrocarbons using spectral uncertainty propagation and minimization techniques, Proc. Combust. Inst. 34 (2013) 527–536.
[11] Y. Xin, D.A. Sheen, H. Wang, C.K. Law, Skeletal reaction model generation, uncertainty quantification and minimization: combustion of butane, Combust. Flame 161 (2014) 3031–3039.
[12] T. Varga, T. Nagy, C. Olm, I.G. Zsély, R. Pálvölgyi, É. Valkó, G. Vincze, M. Cserháti, H.J. Curran, T. Turányi, Optimization of a hydrogen combustion mechanism using both direct and indirect measurements, Proc. Combust. Inst. 35 (2015) 589–596.
[13] C. Olm, T. Varga, É. Valkó, S. Hartl, C. Hasse, T. Turányi, Development of an ethanol combustion mechanism based on a hierarchical optimization approach, Int. J. Chem. Kinet. 48 (2016) 423–441.
[14] V. Samu, T. Varga, K. Brezinsky, T. Turányi, Investigation of ethane pyrolysis and oxidation at high pressures using global optimization based on shock tube data, Proc. Combust. Inst. 36 (2017) 691–698.
[15] A. Gelman, J.B. Carlin, H.S. Stern, D.B. Dunson, A. Vehtari, D.B. Rubin, Bayesian Data Analysis, CRC, New York, 2013.
[16] J. Oakley, A. O'Hagan, Bayesian inference for the uncertainty distribution of computer model outputs, Biometrika 89 (2002) 769–784.
[17] K. Braman, T.A. Oliver, V. Raman, Bayesian analysis of syngas chemistry models, Combust. Theory Modell. 17 (2013) 858–887.
[18] N. Galagali, Y.M. Marzouk, Bayesian inference of chemical kinetic models from proposed reactions, Chem. Eng. Sci. 123 (2015) 170–190.
[19] A. O'Hagan, Bayesian analysis of computer code outputs: a tutorial, Reliab. End. Syst. Safe. 91 (2006) 1290–1300.
[20] H.N. Najm, B.J. Debusschere, Y.M. Marzouk, S. Widmer, O. Le Maître, Uncertainty quantification in chemical systems, Int. J. Numer. Methods Eng. 80 (2009) 789–814.
[21] K. Miki, S.H. Cheung, E.E. Prudencio, P.L. Varghese, Bayesian uncertainty quantification of recent shock tube determinations of the rate coefficient of reaction $H + O_2 \rightarrow OH + O$, Int. J. Chem. Kinet. 44 (2012) 586–597.
[22] L. Hakim, G. Lacaze, M. Khalil, K. Sargsyan, H. Najm, J. Oefelein, Probabilistic parameter estimation in a 2-step chemical kinetics model for n-dodecane jet autoignition, Combust. Theory Modell. 22 (2018) 446–466.
[23] M. Khalil, H.N. Najm, Probabilistic inference of reaction rate parameters from summary statistics, Combust. Theory Modell. 22 (2018) 635–665.
[24] M. Frenklach, A. Packard, G. Garcia-Donato, R. Paulo, J. Sacks, Comparison of statistical and deterministic frameworks of uncertainty quantification, SIAM/ASA J. Uncertain. 4 (2016) 875–901.
[25] D.A. Sheen, H. Wang, The method of uncertainty quantification and minimization using polynomial chaos expansions, Combust. Flame 158 (2011) 2358–2374.
[26] G. Li, C. Rosenthal, H. Rabitz, High dimensional model representation, J. Phys. Chem. A 105 (2001) 7765–7777.
[27] T. Ziehn, A.S. Tomlin, A global sensitivity study of sulfur chemistry in a premixed methane flame model using hdmr, Int. J. Chem. Kinet. 40 (2008) 742–753.
[28] S. Li, B. Yang, F. Qi, Accelerate global sensitivity analysis using artificial neural network algorithm: case studies for combustion kinetic model, Combust. Flame 168 (2016) 53–64.
[29] R. Knutti, T.F. Stocker, F. Joos, G.K. Plattner, Probabilistic climate change projections using neural networks, Clim. Dyn. 21 (2003) 257–272.

[30] C. Balaji, T. Padhi, A new ann driven mcmc method for multi-parameter estimation in two-dimensional conduction with heat generation, Int. J. Heat Mass Transfer 53 (2010) 5440–5455.
[31] L. Cai, H. Pitsch, S.Y. Mohamed, V. Raman, J. Bugler, H. Curran, S.M. Sarathy, Optimized reaction mechanism rate rules for ignition of normal alkanes, Combust. Flame 173 (2016) 468–482.
[32] O. Pajonk, B.V. Rosic, H.G. Matthies, Sampling-free linear bayesian updating of model state and parameters using a square root approach, Comput. Geosci. 55 (2013) 70–83.
[33] D.A. Sheen, Mumpce_py: a python implementation of the method of uncertainty minimization using polynomial chaos expansions, J. Res. Nat. Inst. Stand. Technol. (2017) 122.
[34] B. Sudret, Global sensitivity analysis using polynomial chaos expansions, Reliab. End. Syst. Safe. 93 (2008) 964–979.
[35] A.S. Tomlin, The role of sensitivity and uncertainty analysis in combustion modelling, Proc. Combust. Inst. 34 (2013) 159–176.
[36] J. Prager, H.N. Najm, K. Sargsyan, C. Safta, W.J. Pitz, Uncertainty quantification of reaction mechanisms accounting for correlations introduced by rate rules and fitted arrhenius parameters, Combust. Flame 160 (2013) 1583–1593.
[37] O.P. Le Maître, O.M. Knio, H.N. Najm, R.G. Ghanem, Uncertainty propagation using wiener–haar expansions, J. Comput. Phys. 197 (2004) 28–57.
[38] M.T. Reagan, H.N. Najm, B.J. Debusschere, O.P.L. Maître, O.M. Knio, R.G. Ghanem, Spectral stochastic uncertainty quantification in chemical systems, Combust. Theory Modell. 8 (2004) 607–632.
[39] M.T. Reagan, H.N. Najm, R.G. Ghanem, O.M. Knio, Uncertainty quantification in reacting-flow simulations through non-intrusive spectral projection, Combust. Flame 132 (2003) 545–555.
[40] G. Li, S. Wang, H. Rabitz, S. Wang, P. Jaffè, Global uncertainty assessments by high dimensional model representations (HDMR), Chem. Eng. Sci. 57 (2002) 4445–4460.
[41] T. Ziehn, K.J. Hughes, J.F. Griffiths, R. Porter, A.S. Tomlin, A global sensitivity study of cyclohexane oxidation under low temperature fuel-rich conditions using hdmr methods, Combust. Theory Modell. 13 (2009) 589–605.
[42] A.S. Tomlin, E. Agbro, V. Nevrlý, J. Dlabka, M. Vašinek, Evaluation of combustion mechanisms using global uncertainty and sensitivity analyses: a case study for low-temperature dimethyl ether oxidation, Int. J. Chem. Kinet. 46 (2014) 662–682.
[43] É. Hébrard, A.S. Tomlin, R. Bounaceur, F. Battin-Leclerc, Determining predictive uncertainties and global sensitivities for large parameter systems: a case study for n-butane oxidation, Proc. Combust. Inst. 35 (2015) 607–616.
[44] I. Basheer, M. Hajmeer, Artificial neural networks: fundamentals, computing, design, and application, J. Microbiol. Methods 43 (2000) 3–31.
[45] A.K. Jain, J. Mao, K.M. Mohiuddin, Artificial neural networks: a tutorial, Comput. 29 (1996) 31–44.
[46] M.T. Hagan, M.B. Menhaj, Training feedforward networks with the marquardt algorithm, IEEE Trans. Neural Networks 5 (1994) 989–993.
[47] C. Maschio, D.J. Schiozer, Bayesian history matching using artificial neural network and markov chain monte carlo, J. Pet. Sci. Eng. 123 (2014) 62–71.
[48] S. Chib, E. Greenberg, Understanding the metropolis-hastings algorithm, Am. Stat. 49 (1995) 327–335.
[49] M. Steyvers, Computational Statistics with Matlab, University of California, Irvine, Irvine, 2011.
[50] C. Andrieu, N. de Freitas, A. Doucet, M.I. Jordan, An introduction to MCMC for machine learning, Mach. Learn. 50 (2003) 5–43.
[51] I.A. Basheer, Selection of methodology for neural network modeling of constitutive hystereses behavior of soils, Comput. Aided Civ. Infrastruct. Eng. 15 (2000) 445–463.
[52] D. Atabay, available at <http://pyrenn.readthedocs.io/en/latest/>, 2017.
[53] J. Li, J.-H. Cheng, J.-Y. Shi, F. Huang, Brief Introduction of Back Propagation (bp) Neural Network Algorithm and Its improvement, Advances in Computer Science and Information Engineering, Springer, Berlin, 2012.
[54] S. Hosder, R. Walters, M. Balch, Efficient sampling for non-intrusive polynomial chaos applications with multiple uncertain input variables, 48th AIAA/ASME/ASCE/AHS/ASC Structures, Structural Dynamics and Material Conference (2007), p. 1939.
[55] J. Feinberg, H.P. Langtangen, Chaospy: an open source tool for designing methods of uncertainty quantification, J. Comput. Sci. 11 (2015) 46–57.
[56] G. Li, H. Rabitz, S.W. Wang, P.G. Georgopoulos, Correlation method for variance reduction of monte carlo integration in RS-HDMR, J. Comput. Chem. 24 (2003) 277–283.
[57] O. Park, P.S. Veloo, D.A. Sheen, Y. Tao, F.N. Egolfopoulos, H. Wang, Chemical kinetic model uncertainty minimization through laminar flame speed measurements, Combust. Flame 172 (2016) 136–152.
[58] X. Zhang, G. Wang, J. Zou, Y. Li, W. Li, T. Li, H. Jin, Z. Zhou, Y.-Y. Lee, Investigation on the oxidation chemistry of methanol in laminar premixed flames, Combust. Flame 180 (2017) 20–31.
[59] S. Li, T. Tao, J. Wang, B. Yang, C.K. Law, F. Qi, Using sensitivity entropy in experimental design for uncertainty minimization of combustion kinetic models, Proc. Combust. Inst. 36 (2017) 709–716.
[60] D. Baulch, C. Bowman, C. Cobos, R. Cox, T. Just, J. Kerr, M. Pilling, D. Stocker, J. Troe, W. Tsang, Evaluated kinetic data for combustion modeling: supplement II, J. Phys. Chem. Ref. Data 34 (2005) 757–1397.
[61] J. Wang, S. Li, B. Yang, Combustion kinetic model development using surrogate model similarity method, Combust. Theory Modell. 22 (2018) 777–794.
[62] U. Burke, W.K. Metcalfe, S.M. Burke, K.A. Heufer, P. Dagaut, H.J. Curran, A detailed chemical kinetic modeling, ignition delay time and jet-stirred reactor study of methanol oxidation, Combust. Flame 165 (2016) 125–136.
[63] D.M.N. Goodwin, H. Moffat, R. Speth, available at <http://www.cantera.org/>, 2017.
[64] K. Hsu, H.V. Gupta, S. Sorooshian, Artificial neural network modeling of the rainfall-runoff process, Water Resour. Res. 31 (1995) 2517–2530.
[65] S. Dreiseitl, L. Ohno-Machado, Logistic regression and artificial neural network classification models: a methodology review, J. Biomed. Inform. 35 (2002) 352–359.
[66] C. Andrieu, A. Doucet, R. Holenstein, Particle Markov chain monte carlo methods, J. R. Stat. Soc. 72 (2010) 269–342.
[67] T. Lu, C.K. Law, Toward accommodating realistic fuel chemistry in large-scale computations, Prog. Energy Combust. Sci. 35 (2009) 192–215.